7. Turnshek D A et al. *Astron. J.* **99** 1243 (1990)
8. Thorne K S *Astrophys. J.* **191** 507 (1974)
9. Penrose R *Riv. Nuovo Cimento* (1) 252 (1969), Numero Speziale
10. Blandford R D, Znajek R L *Mon. Not. R. Astron. Soc.* **179** 433 (1977)
11. Fabian A C et al. *Mon. Not. R. Astron. Soc.* **238** 729 (1989)
12. Laor A *Astrophys. J.* **376** 90 (1991)
13. Patrick A R et al. *Mon. Not. R. Astron. Soc.* **411** 2353 (2011)
14. Patrick A R et al. *Mon. Not. R. Astron. Soc.* **416** 2725 (2011)
15. Brenneman L W, Reynolds C S *Astrophys. J.* **702** 1367 (2009)
16. Brenneman L W et al. *Astrophys. J.* **736** 103 (2011)
17. de La Calle Pérez I et al. *Astron. Astrophys.* **524** A50 (2010)
18. Daly R A *Mon. Not. R. Astron. Soc.* **414** 1253 (2011)
19. Silant'ev N A et al. *Astron. Astrophys.* **507** 171 (2009)
20. Meier D L *Astrophys. J.* **522** 753 (1999)
21. Foschini L *Int. J. Mod. Phys. Conf. Ser.* **08** 172 (2012); arXiv: 1107.2785
22. Garofalo D *Astrophys. J.* **699** 400 (2009)
23. Sobolev V V *Uchen. Zap. Leningr. Gos. Univ.* **116** 1 (1949)
24. Chandrasekhar S *Radiative Transfer* (Oxford: Clarendon Press, 1950)
25. Mayer M, Pringle J E *Mon. Not. R. Astron. Soc.* **368** 379 (2006)
26. Bonanno A, Urpin V *Astron. Astrophys.* **473** 701 (2007)
27. Novikov I D, Thorne K S, in *Black Holes* (Eds C DeWitt, B C DeWitt) (New York: Gordon and Breach, 1973) p. 343
28. Crummy J et al. *Mon. Not. R. Astron. Soc.* **365** 1067 (2006)


PACS numbers: 97.10.Bt, 97.80.Jp, 98.70.Qy
DOI: 10.3367/UFNe.0183.201307g.0752

# X-ray binaries and star formation

M R Gilfanov

## 1. Introduction

Progress in X-ray astronomy gave rise to a new method for estimating the star formation rate in distant galaxies using the measurement of their X-ray emission [1, 2]. X-ray observations of nearby galaxies demonstrated that if a galaxy does not show activity from the nucleus (i.e., if the rate of gas accretion onto the central supermassive black hole is low), its X-ray radiation is mainly due to X-ray binaries. Studies of high-mass X-ray binaries in our Galaxy and in nearby galaxies by the X-ray observatories Chandra, XMM-Newton (X-ray Multi-Mirror Misson), INTEGRAL (INTErnational Gamma-Ray Astrophysics Laboratory), and ASCA (Advanced Satellite for Cosmology and Astrophysics), by the Kvant module of the 'Mir' Space Station, etc., have allowed finding the dependence of the number of X-ray binaries on the star formation rate of young stars in these galaxies.

It is well known that neutron stars and black holes are end products of the evolution of stars with masses exceeding $\approx (8-10)\, M_\odot$ (see, e.g., [3, 4]). Accretion onto these compact objects leads to an energy release comparable to their rest mass energy per unit mass of accreting gas, i.e., $L_{\rm X} = \eta\, \dot{M} c^2$, with the efficiency $\eta \sim 0.1-0.2$. If these objects are in binary systems, and the secondary star (typically, a main-sequence star, a subgiant, or a giant) either fills its Roche lobe or intensively loses mass via powerful stellar wind, the accretion of matter from the secondary leads to the appearance of a bright compact X-ray source — an X-ray binary. X-ray binaries are usually subdivided into two classes according to the mass of the donor star: high-mass X-ray binaries (HMXBs) and low-mass X-ray binaries (LMXBs). These two classes are separated by the poorly populated region from $\sim 1\, M_\odot$ to $\sim 5\, M_\odot$, in which there are virtually no bright stationary X-ray sources. The difference in the donor star mass determines the difference in the characteristic time scales of these systems. In the case of massive donors, the longest time scale, which is determined by the nuclear evolution of the star, does not exceed several dozen million years [3]. This scale is comparable with the characteristic duration of a star-formation episode; therefore, it is natural to expect that the number of such systems in a galaxy is proportional to the star formation rate (SFR) [1, 2, 5]:

$$N_{\rm HMXB}\,,\ L_{\rm X,\,HMXB} \propto {\rm SFR}\,. \qquad (1)$$

The evolution of low-mass stars, by contrast, is determined by the rate of loss of orbital angular momentum or the nuclear evolution time scale of the low-mass star, which is usually $\sim 1-10$ billion years [4]. Therefore, it is expected that the number of such systems in a galaxy is determined by the total mass of stars in the galaxy:

$$N_{\rm LMXB}\,,\ L_{\rm X,\,LMXB} \propto M_*\,. \qquad (2)$$

Classical methods of estimation of the star formation rate in a galaxy are based on measurements of the total emission from massive stars. Due to a relatively short lifetime, the number of massive stars in a galaxy can characterize the star formation rate. The radiation from massive stars can be directly measured in the ultraviolet band or by the effect of its interaction with the surrounding interstellar medium, for example, using infrared emission from dust or $\rm H_\alpha$ emission of hydrogen ionized by the ultraviolet emission of massive stars. The link between the luminosity of this radiation and the formation rate of massive stars is determined theoretically using models of population synthesis of stellar evolution (see review [7]).

The need to take corrections due to interstellar absorption into account is a major difficulty of traditional methods. Uncertainties in the parameters of the interstellar medium, its optical depth, and its dust content make the estimation of the fraction of the primary ultraviolet radiation transformed into infrared emission highly uncertain; in particular, this fraction can depend on the type of galaxy and its specific star formation rate. Another difficulty is due to the cosmological redshift, which shifts the emission frequency outside the convenient optical bands; this hampers the application of classical methods to studies of distant galaxies with high redshifts. Therefore, the appearance of a new method, which is based on the X-ray emission of accreting neutron stars and black holes, is important for testing and calibrating traditional methods, as well as for broadening their area of application.

An important feature of the new method is its weaker dependence on the interstellar absorption. Indeed, attenuating a 3 keV emission twofold requires the hydrogen column density (the hydrogen density integrated along the line of

**M R Gilfanov** Space Research Institute, Russian Academy of Sciences, Moscow, Russian Federation
E-mail: gilfanov@iki.rssi.ru

*Uspekhi Fizicheskikh Nauk* **183** (7) 752 – 761 (2013)
DOI: 10.3367/UFNr.0183.201307g.0752
Translated by K A Postnov; edited by A M Semikhatov

sight) $N_{\rm H} \sim 5 \times 10^{22}$ cm$^{-2}$, which corresponds to huge absorption in the optical band ($A_{\rm V} \sim 30$).

Due to the large free path of X-ray photons in a rarefied medium, the X-ray emission from star-forming galaxies played an important role in the ionization balance of the intergalactic medium during the reionization epoch, in particular, in the formation of the hydrogen 21 cm line. To calculate the reionization of the intergalactic medium by the emission from the first stars, galaxies, and quasars, and to interpret observations on the 21 cm hydrogen line, it is critically important to precisely know the specific X-ray emission of star-forming galaxies, $L_{\rm X}/{\rm SFR}$, and its behavior at high redshifts (see review [8]).

Currently, the formation and evolution of X-ray binaries cannot be modeled from first principles. Some critically important evolutionary stages, such as the common envelop stage, are poorly understood, and many initial parameters, including the distribution of masses of companions and orbital periods, are inferred from observations with considerable uncertainty. In theoretical population synthesis calculations (see review [4]), these quantities are described using simplified models and parameters, such as the common envelop efficiency, a flat form of the distribution of the mass ratio of components, etc. Observations of X-ray binary populations in external galaxies, measurements of their specific luminosity, the determination of the relation between the number of sources and the recent star formation history, and the measurement of the X-ray luminosity function of X-ray binaries of different types can directly probe the theory of binary star evolution and test population synthesis models.

X-ray observations of nearby and remote galaxies are required in order to construct the luminosity function of X-ray binaries and to establish the relation between their X-ray luminosity and the star formation rate. To apply this method for high-redshift galaxies, its dependence on redshift should be found. Such observations were carried out in the framework of an extensive program of X-ray studies of galaxies with different morphological types (old and young) [1, 2, 6, 9–13]. Using data obtained by the space observatories Chandra, GALEX (GALaxy Evolution Explorer), Spitzer, and HST (Hubble Space Telescope), and by the 2MASS (Two Micron All Sky Survey) sky survey, more than 100 galaxies of different morphological types were studied in the X-ray, ultraviolet, and far and near infrared bands. These galaxies have stellar populations with different ages and star-formation histories. The main results of these studies are reported in what follows.

## 2. Relation of the X-ray binary population to the star formation rate and the total mass of stars in a galaxy

The simple qualitative picture of the relation between the population of X-ray binaries and the star formation rate, presented in the Introduction, was formulated in the 1970s [5], and the first rough observational tests of this relation were obtained at the early 1990s [14]. However, precise verification of the theory became possible only with the launch of the Chandra X-ray observatory. Due to the high angular resolution of approximately 0.5 arc seconds, which is unique for X-ray astronomy, the Chandra orbital observatory is able to resolve and study populations of compact X-ray sources in external galaxies up to distances of $\sim$ 30–100 Mpc. This feature has allowed 'taking a census' of X-ray binaries in the external galaxies in a way similar to the Milky Way (which was made by instruments with a much coarser angular resolution [15, 16]). In particular, it became possible to construct luminosity functions of compact X-ray sources, to measure their total X-ray luminosity, and to separate the X-ray emission of compact sources from diffuse X-ray radiation of the interstellar gas.

Star-forming galaxies typically also have some relatively old stellar population, including low-mass X-ray binaries whose X-ray emission is not related to the current star formation. In an external galaxy, it is virtually impossible to distinguish a low-mass binary from a high-mass X-ray binary by optical observations, with the exception of the nearest galaxies. The contributions from these two types of X-ray binaries are proportional to the star formation rate and stellar mass, and therefore minimizing the contribution from low-massive binaries requires selecting galaxies with a sufficiently high specific star formation rate. As shown in [1, 2], the threshold value of the specific star formation rate should be ${\rm SFR}/M_* \geqslant 10^{-10}$ yr$^{-1}$.

For our analysis, we selected about 30 nearby galaxies (distances $D \leqslant 40$ Mpc) observed by the Chandra satellite in X-rays, and the GALEX and Spitzer satellites in the respective ultraviolet and infrared bands. The Chandra data were used to determine X-ray fluxes and the total number, luminosities, and luminosity function of compact X-ray sources; the ultraviolet and infrared data were used to estimate the star formation rate as described in [2]. The obtained dependence is shown in Fig. 1a. This figure clearly shows the direct proportionality between the total luminosity of high-mass X-ray binaries and the star formation rate in a given galaxy. The power-law approximation yields $\log L_{\rm X} = \log K + \beta \log {\rm SFR}$ with the best-fit slope $\beta = 1.01 \pm 0.11$, which is consistent with unity [2].

In a similar way, we have selected about 30 nearby early type galaxies (mostly elliptical), in which the age of stellar populations exceeds several billion years and the population of compact X-ray sources mainly includes low-mass X-ray binaries. Using this sample, we studied the relation between the total X-ray luminosity of low-mass X-ray binaries with the total stellar mass $M_*$ of a given galaxy. The result is presented in Fig. 1b, which demonstrates that in this case, too, the data are in good agreement with the linear law $L_{\rm X} \propto M_*$ [6].

Thus, based on the Chandra observations of a large sample of nearby galaxies, we have obtained the following scaling relations for the X-ray luminosity and the number of HMXBs and LMXBs:

$$L_{\rm X,\,HMXB} \approx 2.5 \times 10^{39}\,{\rm SFR}\,, \quad N_{\rm HMXB} \approx 13\,{\rm SFR}\,, \tag{3}$$

$$L_{\rm X,\,LMXB} \approx 1.0 \times 10^{39}\,\frac{M_*}{10^{10} M_\odot}\,, \quad N_{\rm LMXB} \approx 14\,\frac{M_*}{10^{10} M_\odot}\,, \tag{4}$$

where $L_{\rm X}$ is the total X-ray luminosity of the binary population of a given type in the 0.5–8.0 keV range, $N_{\rm X}$ is the number of X-ray binaries with X-ray luminosity exceeding $L_{\rm X} \geqslant 10^{37}$ erg s$^{-1}$, SFR is the star formation rate in units $M_\odot$ yr$^{-1}$, and $M_*$ is the stellar mass of the studied galaxy [1, 2, 6].

## 3. Time evolution of the population of high-mass X-ray binaries

Simple considerations that follow from the theory of formation and evolution of binary systems suggest that the

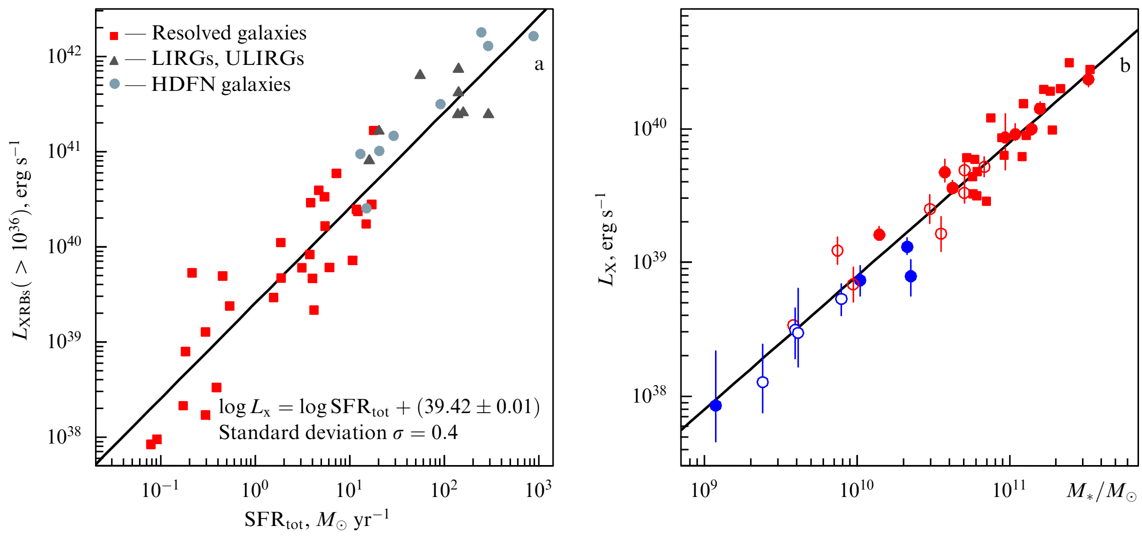


**Figure 1.** The total X-ray luminosity of X-ray binaries as a function of the star formation rate and stellar mass of the host galaxy. (a) Star-forming galaxies in which young stellar population is dominated by high-mass X-ray binaries; the number of high-mass X-ray binaries is proportional to the star formation rate. For comparison, also shown are data for luminous and ultra-luminous infrared galaxies (LIRG — Luminous Infrared Galaxy, ULIRG — Ultra-Luminous Infrared Galaxy) (triangles) and distant star-forming galaxies detected by the Chandra observatory in the Hubble Deep Field North (HDFN) survey (dots). These galaxies have not been resolved by Chandra, and therefore the total luminosity, which includes both X-ray emission from unresolved compact sources and diffuse gas radiation is shown for them. (b) Data for elliptical galaxies in which the star formation ended several billion years ago and only low-mass X-ray binaries remained. Their population is determined by the total stellar mass of the host galaxy. The straight lines show linear fits. (Based on observations of the Chandra X-ray Observatory [2, 6, 12].)

relation between an X-ray binary population and star formation must be more complicated than the purely linear dependence in (3). Indeed, the lifetime of even the most massive stars with a mass $\sim 100 M_\odot$ is $\gtrsim 3$ Myrs. This determines the time of formation of the first black holes in a galaxy. Clearly, X-ray binaries cannot appear earlier than the first compact remnants of stellar evolutions. On the other hand, the lifetime of a star with the mass $8 M_\odot$, the lower mass limit for a neutron star progenitor, is $\approx 40$ Myrs. The longest evolutionary time scale of massive binaries is determined by the lifetime of stars with the mass $\sim 5 M_\odot$, which is $\sim 100$ mln years [17]. Hence, it is natural to expect that the population of high-mass X-ray binaries evolves on the time scale of 100 Myrs.

The number of X-ray binaries that are active at some time $t$ is determined by the total contribution from systems with different ages according to the recent star formation history, $\mathrm{SFR}\,(t-\tau)$, and the function $\eta_{\mathrm{HMXB}}(\tau)$ that describes the dependence of the number or X-ray binaries on time $\tau$ since the moment of star formation:

$$N_{\mathrm{HMXB}}(t) = \int \mathrm{SFR}(t-\tau)\, \eta_{\mathrm{HMXB}}(\tau)\, \mathrm{d}\tau\,. \qquad (5)$$

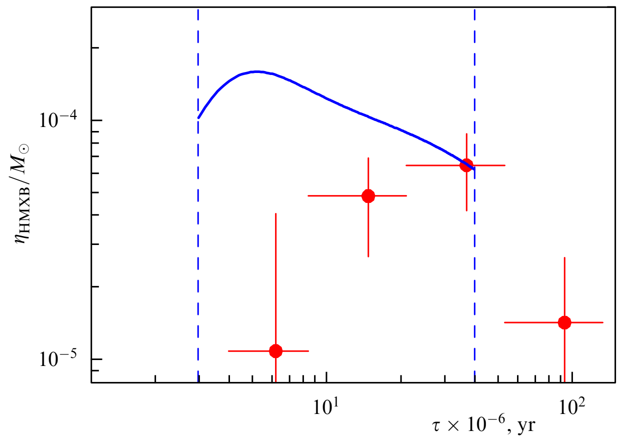


**Figure 2.** The number of high-mass X-ray binaries as a function of time after a star-formation event. The plot is produced using X-ray and optical observations of the Small Magellanic Cloud. The number of high-mass X-ray binaries is normalized by the total mass of massive stars with $M_* \geqslant 8 M_\odot$ formed. The solid curve corresponds to a model based on the rate of supernova explosions. The two vertical dashed lines respectively show the times of the formation of the first black hole and the last neutron star, calculated from the standard theory of single star evolution. (From paper [10].)

Obviously, different star clusters in a galaxy have different star formation histories, and therefore relations (3) may not hold on the angular scales corresponding to individual star-forming regions, and the angular distribution of high-mass X-ray binaries does not correlate with star formation indicators, such as $H_\alpha$ emission distribution [18, 19]. The existence of universal relations (3) is the result of averaging the function $\eta_{\mathrm{HMXB}}(\tau)$ over star forming regions of different ages. At least a fraction of the dispersion of points in the observed relation $L_{\mathrm{X}} - \mathrm{SFR}$ (see Fig. 1) can be due to different age distributions of stellar populations, i.e., due to different star formation histories (another part of the dispersion may be related to different metallicities of star-forming regions [2]).

Comparing the angular distribution of high-mass X-ray binaries with the spatially resolved star formation history in a galaxy, allows determining the function $\eta_{\mathrm{HMXB}}(\tau)$ experimentally. This was first done in [10], where the spatially resolved star formation history of the Small Magellanic Cloud was derived from the photometric survey of Magellanic Clouds [20], and the spatial distribution of high-mass X-ray binaries was determined using XMM-Newton X-ray observations. By solving the inverse problem presented by Eqn (5), the Green's function $\eta_{\mathrm{HMXB}}(\tau)$ shown in Fig. 2 was found.

The obtained dependence significantly differs from type-II supernova explosion rate and is consistent with the general considerations outlined above: the number of high-mass X-ray binaries reaches a maximum 20–50 Myrs after the star formation event, i.e., much later than the maximum of the supernova explosion rate. This is clearly due to the evolution of the companion stars, whose evolutionary time can be as long as $\sim 100$ Myrs for a single star with a mass $\sim 5M_{\odot}$ (ignoring evolutionary effects in a binary system).

When interpreting these results, it should be borne in mind that the function $\eta_{\rm HMXB}(\tau)$ depends on the threshold luminosit, above which X-ray sources are selected. In the analysis by Shtykovsky and Gilfanov [10], a low luminosity threshold was used, so weak X-ray sources (predominantly Be/X-ray binaries) dominate in the sample, and binaries with black holes and O/B donor stars are absent. Due to a sufficiently flat luminosity function (see below), the latter systems determine the total luminosity of the typical star-forming galaxy (see Fig. 1). Because of the shorter lifetime of more massive O/B stars, the characteristic evolutionary time of such systems is smaller, and the corresponding peak of their population will be shifted to earlier times, i.e., the function $\eta_{\rm HMXB}(\tau)$ for brighter sources will have a different form. Unfortunately, experimental determination of this function using the Magellanic Cloud is impossible due to the low star formation rate and the absence of bright X-ray sources (see Section 6), and a similar analysis for galaxies with high star formation rates is more complicated due to difficulties in the determination of the spatially resolved star formation history in remote galaxies.

## 4. Luminosity functions of X-ray binaries

The uniquely high angular resolution of the Chandra X-ray Observatory allows us to construct luminosity functions of X-ray binaries in galaxies, and its sensitivity allows detecting objects with a luminosity as low as $\sim 10^{35}-10^{36}$ erg s$^{-1}$. Observations of a large number of nearby galaxies within $\sim 30$–50 Mpc have shown that luminosity functions of compact X-ray sources in different galaxies have approximately the same shape and differ only by normalization. The shape of luminosity functions in young and old galaxies is different, and the normalization is respectively proportional to the star formation rate and stellar mass. In the first approximation, these findings suggest universal luminosity functions of high-mass and low-mass X-ray binaries. The average luminosity functions are shown in Fig. 3.

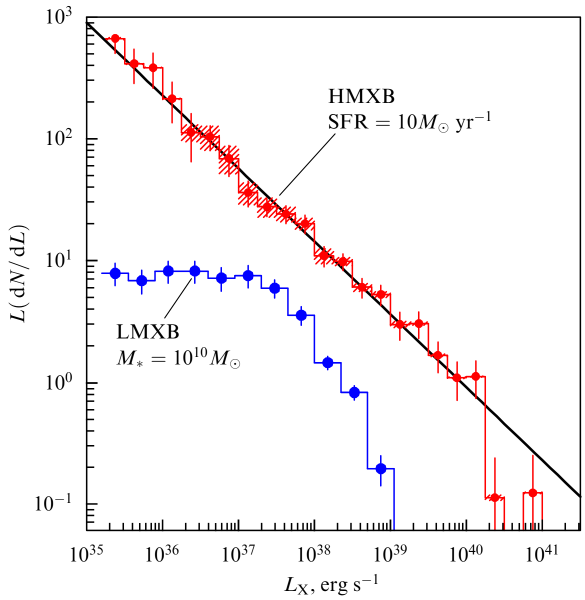


**Figure 3.** Luminosity functions of compact X-ray sources in star-forming (young, HMXB) and elliptical (old, LMXB) galaxies. In star-forming galaxies, high-mass X-ray binaries prevail in the compact X-ray sources population, while in old galaxies, low-mass X-ray binaries dominate. The luminosity functions are respectively normalized by the star formation rate SFR = $10M_{\odot}$ yr$^{-1}$ and the stellar mass $M_* = 10^{10}\,M_{\odot}$. (From papers [2, 6].)

Figure 3 demonstrates that the luminosity functions of high-mass and low-mass X-ray binaries have radically different forms. This is due to different mechanisms of mass transfer in these types of binaries. In most high-mass binaries, accretion onto a compact star proceeds from the stellar wind of a massive optical companion. In this case, the luminosity function of X-ray binaries is mainly determined by the donor mass distribution [21], which leads to the formation of a power-law distribution [1, 2]

$$\frac{\mathrm{d}N_{\rm HMXB}}{\mathrm{d}L_{\rm X}} \propto \mathrm{SFR}\; L_{\rm X}^{-1.6}\,. \qquad (6)$$

In low-mass binaries, the mass exchange between the binary components occurs through the inner Lagrange point due to the Roche lobe overflow. The luminosity function in this case is mainly determined by the orbital parameter distribution of these binaries. This leads to a complex shape of the luminosity function with two breaks at $\log L_{\rm X} \sim 38.5$ and $\log L_{\rm X} \sim 37.0-37.5$. The first break, which occurs close to the Eddington luminosity for neutron stars, is apparently due to the existence of the limit luminosity of accreting neutron stars. Compact objects in systems with higher luminosity are black holes, and their number in the population is significantly smaller. The nature of the second break in the luminosity function remains uncertain. One possibility was suggested in [22]. From an analysis of a galactic sample of low-mass X-ray binaries, the authors of [22] concluded that donors in smaller-luminosity systems, $\log L_{\rm X} \leqslant 37.0-37.5$, are predominantly main-sequence stars, while those in higher-luminosity systems are giant stars. The comparatively short lifetime of giants can be the reason for the steepening of the luminosity function.

## 5. Ultra-luminous X-ray sources

It is surprising that the luminosity function of high-mass X-ray binary systems continues up to the luminosities $\log L_{\rm X} \sim 40.0-40.5$ with the same slope (see Fig. 3). Notably, unlike the luminosity function of low-mass X-ray binaries, this function does not show noticeable features at the Eddington luminosity for neutron stars ($\log L_{\rm X} \sim 38.3$) and stellar-mass black holes ($\log L_{\rm X} \sim 39.0-39.5$). On the other hand, the luminosity function cuts off at $\log L_{\rm X} \approx 40.0-40.5$ (Fig. 4), which corresponds to the Eddington luminosity of an object with a mass of $\sim (50-100)\,M_{\odot}$.

It is well known that the standard evolution of solar-metallicity stars cannot produce black holes with masses higher than $\approx (10-15)\,M_{\odot}$, and the formation of more massive black holes with masses higher than $\sim 100\,M_{\odot}$ is possible from zero-metallicity stars [23]. In principle, it is possible that the brightest X-ray sources are related to

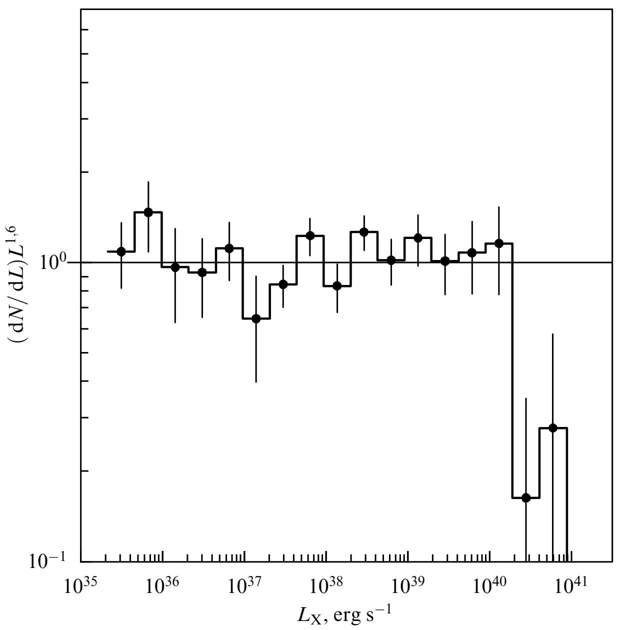


**Figure 4.** Detailed form of the luminosity function of compact X-ray sources in star-forming galaxies. Plotted is the ratio of the luminosity function to the power-law with index 1.6. The normalization is arbitrary. (From paper [2].)

accretion onto such massive black holes (so-called intermediate-mass black holes), which can be the result of the evolution of so-called Population III stars — the first stars in the Universe formed at high redshifts from matter with primordial chemical abundance, with almost zero metals. The relative frequency of the occurrence of such systems must be significantly lower than for the usual massive X-ray binaries with neutron stars and stellar-mass black holes. Therefore, the luminosity function should show a break when passing to systems with intermediate-mass black holes [1]. But the observed luminosity function can be fit by a single power law at all luminosities up to $\log L_{\mathrm{X}} \sim 40$ (see Figs 3, 4). Therefore, systems with $\log L_{\mathrm{X}} \lesssim 40$ most likely contain 'usual' stellar-mass black holes and represent the 'tail' of mass and accretion rate distributions. We note that the standard accretion theory allows luminosities as high as several times the Eddington limit [1, 24, 25]. The cut-off of the luminosity function at $\log L_{\mathrm{X}} \geqslant 40.5$ (see Fig. 4) may correspond to the transition to another population of X-ray sources. Several known sources with $\log L_{\mathrm{X}} \geqslant 40.5$ can be more exotic objects, for example, intermediate-mass black holes produced by the evolution of the first Population III stars.

To conclude this section, we stress that although the outlined picture seems to be quite plausible, no solid confirmation of this concept has been obtained so far. Despite intensive multiwavelength studies of ultra-luminous X-ray sources, their nature remains puzzling [25].

## 6. Limiting luminosity of sources and linearity of the $L_{\mathrm{X}}$–SFR relation

We note a paradoxical, at first glance, fact: the linear dependence of the total X-ray luminosity of high-mass binaries and the star formation rate is a direct consequence of the luminosity function cut-off [26]. This is related to properties of the probability density distribution for the collective luminosity of objects distributed according to relation (6).

If the measured value is the sum of luminosities of a finite number of discrete sources (in contrast, for example, to the luminosity of a gas region),

$$L_{\mathrm{tot}} = \sum_{k=1}^{k=N} L_k \,, \tag{7}$$

then the intuitively obvious relation

$$\langle L_{\mathrm{tot}} \rangle = \int_0^{+\infty} L \, \frac{\mathrm{d}N}{\mathrm{d}L} \, \mathrm{d}L \propto \mathrm{SFR} \tag{8}$$

does not describe the result of measurements of X-ray emission from an arbitrarily chosen galaxy. The most probable value of the luminosity of a given galaxy is predicted by the maximum of the probability distribution $p(L_{\mathrm{tot}})$ (the so-called probability distribution mode), while the expectation value determined by Eqn (8) describes the average result of measurements of a large number of galaxies. Clearly, for a symmetric distribution, for example, a Gaussian one, these two values coincide. But the shape of the distribution $p(L_{\mathrm{tot}})$ is determined by the shape of the luminosity function and can be strongly asymmetric.

We consider an example. The most probable value of the luminosity of the brightest source $\tilde{L}_{\max}$ is determined by the relation

$$N(L > \tilde{L}_{\max}) = \int_{\tilde{L}_{\max}}^{+\infty} \frac{\mathrm{d}N}{\mathrm{d}L} \, \mathrm{d}L \sim 1 \,. \tag{9}$$

For a power-law luminosity function with the slope $\alpha$ and a cut-off at $L_{\mathrm{cut}}$, we obtain

$$\begin{aligned} &\tilde{L}_{\max} \propto \mathrm{SFR}^{\,1/(\alpha-1)} \quad \text{at low SFR} \,, \\ &\tilde{L}_{\max} = L_{\mathrm{cut}} \quad \text{at high SFR} \,. \end{aligned} \tag{10}$$

As expected, the luminosity of the brightest source increases with the star formation rate (the larger the number of sources is in the sample, the higher the probability of finding a bright source from the luminosity function tail). But the luminosity cannot exceed the limiting value $L_{\mathrm{cut}}$; therefore, at high star formation rates, the value $\tilde{L}_{\max}$ stops increasing. These two regimes are separated by the threshold value of the star formation rate, determined by the relation $N(L \sim L_{\mathrm{cut}}) \sim 1$; when this relation holds, we can expect to find several sources with luminosities close to the maximum possible value $L_{\mathrm{cut}}$.

The most probable value of the total luminosity $\tilde{L}_{\mathrm{tot}}$ can be calculated by integrating the luminosity function from $L_{\min}$ to $\tilde{L}_{\max}$:

$$\tilde{L}_{\mathrm{tot}} \approx \int_{L_{\min}}^{\tilde{L}_{\max}} \frac{\mathrm{d}N}{\mathrm{d}L} \, L \, \mathrm{d}L \,. \tag{11}$$

For $1 < \alpha < 2$ and $L_{\min} \ll \tilde{L}_{\max}$, we obtain

$$\tilde{L}_{\mathrm{tot}} \propto \begin{cases} \mathrm{SFR}^{1/(\alpha-1)} & \text{at low SFR} \,, \\ \mathrm{SFR} & \text{at high SFR} \,. \end{cases} \tag{12}$$

For the luminosity function slopes $1 < \alpha < 2$, the total luminosity of a galaxy is determined by the brightest sources in the galaxy, whose luminosity at low star formation rates increases nonlinearly [see formula (12)]. This leads to a nonlinear behavior of $\tilde{L}_{\rm tot}$, which continues until the maximum possible luminosity $L_{\rm cut}$ is reached. A further increase in the star formation rate leads to a linear increase in the number of brightest sources in the galaxy, but not to an increase in their luminosity. Correspondingly, the dependence $L_{\rm X}$ becomes linear. We note that the nonlinear regime is characterized by a large asymmetric dispersion. This problem is considered in paper [26] in more detail.

For parameters of the luminosity function of massive binaries at low star formation rates, we expect to have $L_{\rm X} \propto {\rm SFR}^{1.7}$, and the transition to the linear regime to occur at ${\rm SFR} \sim 10 M_{\odot}$ yr$^{-1}$. However, Fig. 1 does not show such a nonlinear behavior at low SFR. This is because the low-SFR part of Fig. 1 is populated by nearby galaxies, whose sample is not random. These galaxies were selected because they appeared interesting to X-ray astronomers for some reason (for example, because they have bright X-ray sources), i.e., they are subject to the so-called observer bias. In other, more objective, samples of galaxies, the nonlinear dependence of $L_{\rm X}$ on the SFR is clearly seen (for example, in [1, 26]). The sample of galaxies in the deep X-ray Chandra surveys is objective (i.e., all star-forming galaxies in some field were selected), but in all of them ${\rm SFR} \geqslant 10 M_{\odot}$ yr$^{-1}$, which corresponds to a linear dependence of $L_{\rm X}$ on SFR.

It is important to note that the agreement of normalizations of the $L_{\rm X}-{\rm SFR}$ relation for nearby galaxies selected from archival data and for remote galaxies from the deep Chandra surveys suggests, first, that observer bias does not significantly shift the common normalization in this relation. Second, the linear dependence of $L_{\rm X}$ on the SFR at ${\rm SFR} \geqslant 10 M_{\odot}$ per year evidences the fact that the luminosity function of X-ray binaries has a cut-off at $\log L_{\rm X} \leqslant 40-41$. Third, this proves that the maximum luminosity of ultra-luminous X-ray sources at redshifts $z \sim 1$ and star formation rates ${\rm SFR} \sim 100 M_{\odot}$ per year did not substantially exceed luminosities observed in the local Universe. In other words, at high redshifts, there were no significant populations of exotic objects comparable in number to 'ordinary' high-mass X-ray binaries.

## 7. Consequences for the theory of binary star evolution

Observations of populations of X-ray binaries in external galaxies open up the possibility of experimental testing of assumptions underlying the theory of formation and evolution of binary stellar systems. Clearly, a direct way of such testing is the comparison of the observed number of X-ray binaries and their luminosity function with the results of population synthesis calculations.

On the other hand, it is possible to formulate several simple consequences from the experimental results presented above. With the known relation between the number of massive X-ray binaries and the star formation rate, we can estimate the fraction of compact objects becoming X-ray sources due to the accretion of matter in massive binary systems. Our observations imply that the number of X-ray binaries with the luminosity above $10^{35}$ erg s$^{-1}$ is

$$N_{\rm HMXB}(> 10^{35}\ {\rm erg\ s}) \approx 135\,{\rm SFR}\,. \tag{13}$$

On the other hand, this number can be expressed in terms of the formation rate of compact objects $\dot{N}_{\rm co}$ and the mean lifetime of X-ray sources $\bar{\tau}_{\rm X}$:

$$N_{\rm HMXB} \sim \dot{N}_{\rm co} \sum_k f_{{\rm X},k}\, \tau_{{\rm X},k} \sim \dot{N}_{\rm co} f_{\rm X}\, \bar{\tau}_{\rm X}\,. \tag{14}$$

The formation rate of compact objects is approximately equal to the birth rate of massive stars: $\dot{N}_{\rm co} \approx \dot{N}_*(M > 8\, M_{\odot})$. Assuming the Salpeter initial stellar mass function, we obtain

$$\dot{N}_*(M > 8\, M_{\odot}) \approx 7.4 \times 10^{-3}\,{\rm SFR}\,. \tag{15}$$

The summation in Eqn (14) is performed over different types of binaries, including systems with supergiants and Be/X-ray binaries. The coefficient $f_{{\rm X},k}$ is the fraction of compact objects formed in a galaxy that became X-ray sources due to the accretion of matter in the given type of binary system; accordingly, $\tau_{{\rm X},k}$ is the duration of the X-ray stage. The summ $f_{\rm X} = \sum_k f_{{\rm X},k}$ is the total fraction of compact objects that became X-ray sources and $\bar{\tau}_{\rm X}$ is the mean duration of the X-ray phase.

It is known from the theory of evolution of binary systems that for systems with supergiants, $\tau_{\rm X} \sim 10^4$ years and for Be/X-ray binaries, $\tau_{\rm X} \sim 10^5$ years. From observations of our Galaxy and the Magellanic Clouds, we know that most of the massive X-ray binaries with low luminosity, which mostly contribute to the number of sources in relation (13), are Be/X-ray binaries [27]. If this is correct for star-forming galaxies in general, the characteristic duration is $\bar{\tau}_{\rm X} \sim 10^5$ years, and therefore

$$f_{\rm X} \sim 0.18 \left( \frac{\bar{\tau}_{\rm X}\ [{\rm yrs}]}{10^5} \right)^{-1}. \tag{16}$$

The quantity $f_{\rm X}$ is the fraction of compact objects that became X-ray sources due to accretion in massive binary systems during the first 100 Myrs after their formation. In counting the number of X-ray binaries in relation (13), we have used the low luminosity threshold, and hence this population is dominated by Be/X-ray binaries with neutron stars. Therefore, $f_{\rm X}$ characterizes the efficiency of formation of X-ray binaries with neutron stars.

To estimate the formation efficiency of bright accreting black holes, we can repeat the above calculations with the luminosity threshold $10^{39}$ erg s$^{-1}$, which significantly exceeds the Eddington limit for neutron stars. Furthermore, in Eqn (15), we increase the mass limit to $25 M_{\odot}$, i.e., to the minimal mass of the zero-age main sequence star that is capable of producing a black hole at the end of its evolution. We also take into account that the brightest sources apparently have supergiant donor stars for which the characteristic duration of the X-ray phase is $\sim 10^4$ years. As a result, we obtain the relation:

$$f_{\rm X}^{\rm ULX} \sim 3.5 \times 10^{-2} \left( \frac{\bar{\tau}_{\rm X}\ [{\rm yrs}]}{10^4} \right)^{-1}. \tag{17}$$

Hence, a few percent of all stellar-mass black holes produced in a galaxy can become bright X-ray sources that form the population of ultra-luminous X-ray sources with luminosities $\geqslant 10^{39}$ erg s$^{-1}$. We note that in deriving Eqns (16) and (17), we have assumed a Salpeter initial stellar mass function, while it is well known that the initial stellar mass function is flatter for masses $M \leqslant M_{\odot}$. This assumption was made to provide consistency with the determination of the star formation rate, which is normalized to the Salpeter initial mass function [7].

Clearly, the following inequality should hold:

$$f_{\rm X} \leqslant f_{\rm bin}(m_2 \geqslant 5M_\odot)\,, \tag{18}$$

where $f_{\rm bin}(m_2 \geqslant 5M_\odot)$ is the fraction of binary stars in which the mass of the optical companion is above $5M_\odot$. This allows putting bounds on the mass distribution of donor stars in massive binary systems. First, it is possible to immediately exclude the possibility that their distribution is described by a Salpeter mass function, which is independent of the primary star mass. Indeed, in that case, the fraction of binary systems with companion masses above $5M_\odot$ would be $f(m > 5M_\odot) \approx \approx 5.5\times 10^{-3}$, i.e., $\sim 40$ times smaller than the value $f_{\rm X} \sim 0.2$ determined by Eqn (16). Considering power-law mass distributions with arbitrary slopes $\psi(m) \propto m^{-\gamma}$ and assuming $f_{\rm X} = 0.2$, from Eqn (18), we can constrain the mass function slope at $\gamma < 0.3$, which is significantly flatter than the Kroupa or Salpeter mass functions that have a slope $\approx 2.35$ at high masses. Relation (18) also agrees with the flat binary mass ratio distribution [2].

To conclude this section, we note that similar considerations applied to low-mass X-ray binaries result in an extremely low formation efficiency of such objects: $f_{\rm X,\,LMXB} \sim 10^{-6}$ [2]. This must be mainly due to the destruction of a significant fraction of low-mass binary systems by supernova explosions, during which compact objects are formed.

## 8. Contribution of star-forming galaxies to the cosmic X-ray background. Evolution of the $L_{\rm X}$SFR relation

Deep X-ray sky surveys have shown that about 80–90% of the cosmic X-ray background is due to emission from accreting supermassive black holes in active galactic nuclei and quasars [28]. Although with the sensitivity $F_{\rm X} \approx 10^{-17}$ erg s$^{-1}$ cm$^{-2}$ of the deepest X-ray surveys carried out by the Chandra Observatory, the number of star-forming galaxies is less than $\approx 1/4$ of all detected sources, the extrapolation of the source counts indicates that star-forming galaxies should dominate in future sky surveys, which will be 2–5 times deeper [28]. Therefore, their emission must significantly contribute to the cosmic X-ray background and be comparable to its currently unresolved part.

This fraction can be calculated theoretically if the specific X-ray luminosity associated with star formation $c_{\rm X}(z) = L_{\rm X}/{\rm SFR}$ and the star formation rate in the Universe at different redshifts $\dot\rho_*(z)$ are known:

$$S_{\rm tot} = \frac{1}{4\pi}\,\frac{c}{H_0}\int_0^{z_{\max}} \frac{{\rm d}z}{(1+z)^2\,E(z)}\,\dot\rho_*(z)\,c_{\rm X}(z)\,, \tag{19}$$

where $E(z) = \sqrt{\Omega_{\rm m}(1+z)^3 + \Omega_\Lambda}$. Such calculations performed in [29] showed that the contribution of star-forming galaxies to the cosmic X-ray background in the soft X-ray band of 1–2 keV amounts to $\sim 8-12\%$. In the harder X-ray band (2–8 keV), their contribution falls in the range from a few percent to $\sim 20\%$, depending on the assumption about the shape of the spectrum of ultra-luminous X-ray sources at energies of $\sim 20-30$ keV, which is presently unknown. Hence, the contribution of star-forming galaxies, at least in the soft X-ray band, is close to the brightness of the unresolved cosmic X-ray background.

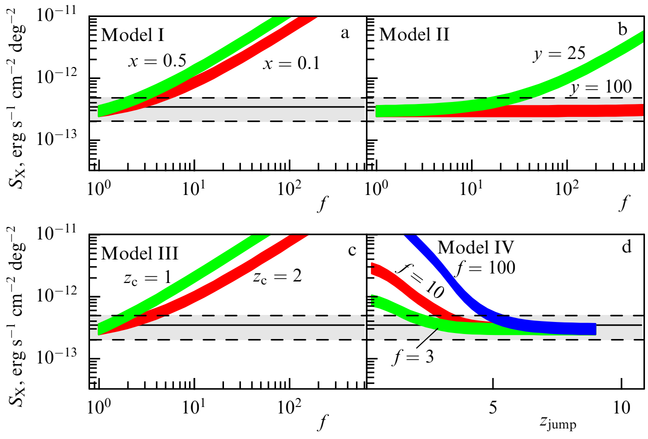


**Figure 5.** X-ray fluxes from star-forming galaxies. The solid horizontal line shows the level of the unresolved X-ray background, the shaded area between the dashed lines shows the 68%-error interval. Different curves correspond to different assumptions about the evolution of the ratio $c_{\rm X} = L_{\rm X}/{\rm SFR}$ with redshift: a jump $c_{\rm X} \to f c_{\rm X}$ at (a) ${\rm SFR} \leqslant x$, (b) ${\rm SFR} \geqslant y$, (c) $z \geqslant z_{\rm c}$, and (d) $z \geqslant z_{\rm jump}$. (From [29].)

Clearly, this fact can be used to constrain the possible redshift evolution of the specific X-ray luminosity associated with star formation, $L_{\rm X}/{\rm SFR}$. Indeed, if high-redshift galaxies had higher $L_{\rm X}/{\rm SFR}$ ratios, then their total luminosity would exceed the brightness of the unresolved background, which is impossible. This is illustrated in Fig. 5, which demonstrates the contribution from star-forming galaxies to the brightness of the background under different assumptions about the dependence of the $L_{\rm X}/{\rm SFR}$ ratio on redshift or the star formation rate. It can be seen from the figure that even for a relatively small (by about a factor of two) increase of $L_{\rm X}/{\rm SFR}$ at $z \approx 2$ or at a low SFR, the predicted contribution of star-forming galaxies to the brightness of the cosmic X-ray background exceeds its unresolved part. Hence, in this redshift interval, the specific X-ray luminosity of star formation never exceeded the local Universe value by more than a factor of $\sim 2$. This conclusion agrees with the properties of ultra-luminous sources at $z \sim 1-2$, discussed in Section 6. On the other hand, these considerations do not significantly constrain the $L_{\rm X}/{\rm SFR}$ behavior at high star formation rates or high redhsifts $z \geqslant 5$. We note that the regime of high star formation rates is well constrained by direct measurements of the $L_{\rm X}/{\rm SFR}$ ratio (Fig. 6).

## 9. Measurement of the galactic star formation rate from X-ray luminosity

In addition to emission from X-ray binaries, the total X-ray luminosity of a galaxy includes emission from hot ionized gas with a temperature of several million Kelvins. X-ray binaries and the hot gas determine the X-ray luminosity of a galaxy if it does not have an active nucleus. Observations of nearby galaxies by the Chandra Observatory showed that the gas provides about 1/4 of the observed X-ray emission from a star-forming galaxy in the 0.5–8.0 keV range, and its luminosity is proportional to the star formation rate, as well as is the luminosity of massive X-ray binaries [30]. Clearly, in distant galaxies at distances greater than 100 Mpc, it is impossible to separate the emission from compact sources

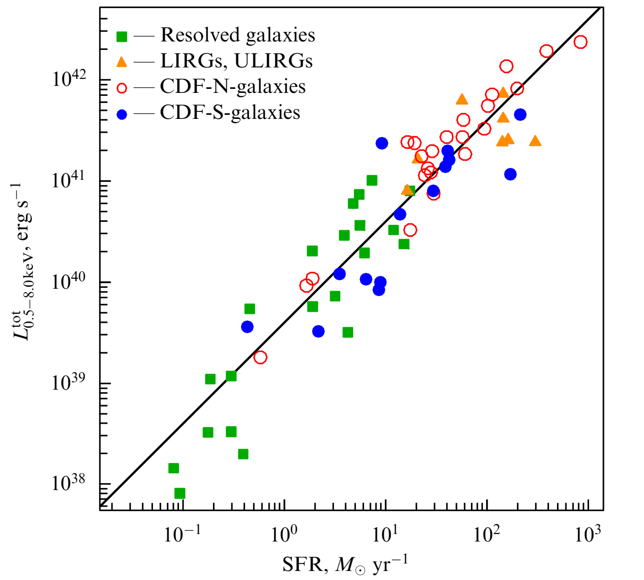


**Figure 6.** The total X-ray luminosity of star-forming galaxies as a function of the star formation rate. Different symbols show nearby galaxies resolved by the Chandra Observatory (squares), luminous and ultraluminous infrared galaxies (triangles), and star-forming galaxies in the North (light circles) and South (dark circles) Chandra deep fields (Chandra Deep Field North (CDF-N), Chandra Deep Field South (CDF-S)). The last ones are located at redshifts $z \approx 0.1-1.3$. The solid straight line shows a linear approximation for the nearby galaxies. (From [13].)

from the diffuse gas emission; therefore, the observations register the total X-ray luminosity of a galaxy. As expected, the total X-ray luminosity of distant galaxies is proportional to the star formation rate [13]. This fact is illustrated in Fig. 6, which shows both nearby galaxies resolved by the Chandra Observatory and distant galaxies discovered in the Deep Chandra South and North Fields [28, 31] at redshifts $z \sim 0.1-1.3$. The figure also shows the linear fit to the data. We note that the approximations for nearby and distant galaxies found in the Chandra deep fields are fully consistent with each other; therefore, we can suggest that a linear relation between the X-ray luminosity of a galaxy and its star formation rate holds up to redshifts $z \approx 1.3$ at least. The dispersion of points relative to the linear fit (the root mean square variance) is rms $\approx 0.4$. As shown in [2], this dispersion cannot be due to systematic or statistical errors and has a physical origin, and is mainly caused ty variations of elemental abundances and differences in the star formation histories of galaxies.

The correlation between the total X-ray luminosity and the star formation rate opens up the key possibility of measuring the star formation rate using its X-ray emission:

$$\mathrm{SFR} = \frac{L_{\rm X}}{3.5 \times 10^{39}\ \mathrm{erg\,s^{-1}}}\ M_\odot\ \mathrm{yr}^{-1}\,. \tag{20}$$

This relation is calibrated using direct observations in the redshift range $z = 0-1.3$. An analysis of the contribution of X-ray binaries to the cosmic X-ray background leads to the conclusion that this relation can be applied up to redshifts $z \sim 2-3$ [29]. We note that the forthcoming all-sky survey by eROSITA (extended ROentgen Survey with an Imaging Telescope Array) by the Spectrum–Roentgen–Gamma observatory will test relation (20) using a sample of $\approx 10^4$ star-forming galaxies [32].

The main source of systematic errors in measuring the star formation rate in galaxies using relation (20) is the contribution of X-ray emission from an accreting central supermassive black hole. An active galactic nucleus with a moderate luminosity $L_{\rm X} \sim 10^{42}$ erg s$^{-1}$ can bias the SFR measurement of the star formation rate, even in a galaxy with a high SFR of the order of $100 M_\odot$ yr$^{-1}$. Because the bright X-ray emission from galaxies is typically due to their nuclear activity, measurements of the SFR using X-ray emission are possible for a relatively small fraction of bright galaxies after a careful search for active nuclei and determination of the morphological type of the galaxies. On the other hand, studies of deep X-ray surveys [28, 31] suggest that the vast majority of faint galaxies with fluxes $F_{\rm X} \leqslant 10^{-17}$ erg s$^{-1}$ are star-forming galaxies at redshifts $z \sim 1-3$. For these galaxies, X-ray emission is a powerful tool for diagnostics of the star formation, and this method can be applied to a large number of galaxies in order to study the star formation history in the Universe. One of the first applications of this method is presented in [33].

## 10. Conclusion

X-ray emission of the majority of galaxies in the observable part of the Universe is due to X-ray binaries — accreting neutron stars and black holes in close binary systems. Their population is determined by the entire history of star formation of the host galaxy, and in the first approximation by its mass and the star formation rate.

X-ray observations of nearby galaxies by the Chandra and XMM-Newton space observatories demonstrated that the luminosity distributions of X-ray binaries in the first approximation are described by universal luminosity functions (see Fig. 3). The total number of compact sources and their total luminosity in star-forming (young) and elliptical (old) galaxies are respectively proportional to the star formation rate and the stellar mass (see Fig. 1). The luminosity functions of compact stars in young and old galaxies are radically different, which is related to different regimes of mass accretion in high-mass and low-mass X-ray binaries. The luminosity function of high-mass X-ray binaries is described by a power-law with the exponent $\approx 1.6$ in the wide range of luminosities $\log L_{\rm X} \sim 35-40$. It shows no features corresponding to Eddington luminosities for neutron stars or stellar-mass black holes, but demonstrates a cut-off at $\log L_{\rm X} \sim 40.0-40.5$ (see Fig. 4). The shape of the luminosity function suggests that most of the galactic ultra-luminous X-ray sources are products of the standard evolution of binary stars and populate the tail of the mass and accretion rate distributions. Much rarer sources with higher luminosity $\log L_{\rm X} \geqslant 40-41$ can be more exotic objects, for example, intermediate-mass black holes, which are products of the evolution of high-mass Population III stars. The linearity of the $L_{\rm X}-$SFR relation in a wide range of redshifts implies that the luminosity function of compact X-ray sources at redshifts $z \sim 1$ and for star formation rates several times higher than in typical nearby galaxies is not significantly different from the local luminosity function.

The specific number of high-mass X-ray binaries per unit star formation rate suggests that a significant fraction of compact objects becomes accreting X-ray sources during the first $\sim 100$ Myrs after their birth [see relation (16)]. This explains the unexpectedly large ($\sim 8-10\%$) contribution of accreting stellar-mass black holes to the brightness of the cosmic X-ray background.

The universal relation between the X-ray luminosity of a galaxy and its rate of formation of massive stars allows estimating the star formation rate in a galaxy from its X-ray luminosity. The $L_{\mathrm{X}}-\mathrm{SFR}$ relation has a relatively small dispersion and was calibrated in a wide range of redshifts, which provides a new tool for determining the star formation rate based on X-ray luminosity of galaxies. This method is independent of traditional star-formation diagnostics based on infrared and ultraviolet observations. It can be used to measure the star formation rate in distant galaxies at $z \sim 1-3$, which should be the dominant population of X-ray sources in future next-generation sky surveys. It may become an efficient tool for measuring the star formation history in the Universe in a wide range of redshifts.

## References


1. Grimm H-J, Gilfanov M, Sunyaev R *Mon. Not. R. Astron. Soc.* **339** 793 (2003)
2. Mineo S, Gilfanov M, Sunyaev R *Mon. Not. R. Astron. Soc.* **419** 2095 (2012)
3. Verbunt F, van den Heuvel E P J, in *X-Ray Binaries* (Cambridge Astrophys. Ser., 26, Eds W H G Lewin, J van Paradijs, E P J van den Heuvel) (Cambridge: Cambridge Univ. Press, 1995) p. 457
4. Postnov K A, Yungelson L R *Living Rev. Relativity* **9** 6 (2006)
5. Sunyaev R A, Tinsley B M, Meier D L *Comments Mod. Phys. C Comments Astrophys.* **7** (6) 183 (1978)
6. Gilfanov M *Mon. Not. R. Astron. Soc.* **349** 146 (2004)
7. Kennicutt R C (Jr.) *Annu. Rev. Astron. Astrophys.* **36** 189 (1998)
8. Furlanetto S R, Peng Oh S, Briggs F H *Phys. Rep.* **433** 181 (2006)
9. Gilfanov M, Grimm H-J, Sunyaev R *Mon. Not. R. Astron. Soc.* **347** L57 (2004)
10. Shtykovskiy P E, Gilfanov M R *Astron. Lett.* **33** 437 (2007) [*Pis'ma Astron. Zh.* **33** 492 (2007)]
11. Voss R, Gilfanov M *Astron. Astrophys.* **447** 71 (2006)
12. Zhang Z, Gilfanov M, Bogdán Á *Astron. Astrophys.* **546** A36 (2012)
13. Mineo S, Gilfanov M, Lehmer B, Sunyaev R *Mon. Not. R. Astron. Soc.* (2013), in press
14. David L P, Jones C, Forman W *Astrophys. J.* **388** 82 (1992)
15. Grimm H-J, Gilfanov M, Sunyaev R *Astron. Astrophys.* **391** 923 (2002)
16. Lutovinov A et al. *Astron. Astrophys.* **444** 821 (2005)
17. Hurley J R, Pols O R, Tout C A *Mon. Not. R. Astron. Soc.* **315** 543 (2000)
18. Shtykovskiy P, Gilfanov M *Astron. Astrophys.* **431** 597 (2005)
19. Shtykovskiy P E, Gilfanov M R *Astron. Lett.* **33** 299 (2007) [*Pis'ma Astron. Zh.* **33** 340 (2007)]
20. Zaritsky D et al. *Astron. J.* **123** 855 (2002)
21. Postnov K A *Astron. Lett.* **29** 372 (2003) [*Pis'ma Astron. Zh.* **29** 424 (2003)]
22. Revnivtsev M, Postnov K, Kuranov A, Ritter H *Astron. Astrophys.* **526** A94 (2011)
23. Zhang W, Woosley S E, Heger A *Astrophys. J.* **679** 639 (2008)
24. Shakura N I, Sunyaev R A *Astron. Astrophys.* **24** 337 (1973)
25. Fabrika S N et al. *Phys. Usp.* **49** 324 (2006) [*Usp. Fiz. Nauk* **176** 339 (2006)]
26. Gilfanov M, Grimm H-J, Sunyaev R *Mon. Not. R. Astron. Soc.* **351** 1365 (2004)
27. Liu Q Z, van Paradijs J, van den Heuvel E P J *Astron. Astrophys.* **455** 1165 (2006)
28. Lehmer B D et al. *Astrophys. J.* **752** 46 (2012)
29. Dijkstra M, Gilfanov M, Loeb A, Sunyaev R *Mon. Not. R. Astron. Soc.* **421** 213 (2012)
30. Mineo S, Gilfanov M, Sunyaev R *Mon. Not. R. Astron. Soc.* **426** 1870 (2012)
32. Xue Y Q et al. *Astrophys. J. Suppl.* **195** 10 (2011)
31. Prokopenko I G, Gilfanov M R *Astron. Lett.* **35** 294 (2009) [*Pis'ma Astron. Zh.* **35** 330 (2009)]
33. Cowie L L, Barger A J, Hasinger G *Astrophys. J.* **748** 50 (2012)


PACS numbers: **07.87.+v**, **96.12.–a**, 96.30.Gc
DOI: 10.3367/UFNe.0183.201307h.0762

# Space-based spectroscopy of Mars: new methods and new results

O I Korablev

## 1. Current Mars problems

After the breakthrough Viking Mars mission in 1972 and a long interruption in Mars studies caused, on the one hand, by the negative result of experiments searching for evidence of life and, on the other hand, by a number of failures of space programs, spacecraft exploration of Mars is currently being extensively and apparently thoroughly performed. Three orbiters are currently operating in Mars orbit: Mars Odyssey (entered Mars orbit in 2001) [1], Mars Express (arrived in orbit in 2003), and Mars Reconnaissance Orbiter (MRO) (entered orbit in 2005) [2]. On the surface of Mars, the Opportunity Rover is still active [3] and the Curiosity Rover recently began to operate [4].

Among the key results obtained after the Viking mission, first of all using Mars Global Surveyor (MGS) (1998–2006), Mars Odyssey, and Mars Express spacecraft, are the discovery of the remanent magnetization of Mars's crust [5], the global altimetry of Mars and the determination of its figure [6], the global mapping of Mars and dating of its geological units [7, 8], and the discovery and global mapping of subsoil water [9, 10]. Nevertheless, a number of important scientific problems concerning both fundamental questions and Mars exploration in the future remain to be solved or are in the process of accumulation and refinement of knowledge.

Three main groups of scientific problems can be distinguished: (1) inner structure of the planet and its volcanism; (2) climate evolution and the current climate of Mars; and (3) the past and current habitability of Mars.

Modern models of Mars's interior cannot answer questions about the thickness and composition of its crust, the composition of the mantle (the enrichment of the mantle of Mars with iron compared to that of Earth) and its inhomogeneities, and the size and structure of Mars's core [11]. Mars shows many signs of volcanic activity, in particular, Olympus Mons, the tallest volcano in the Solar System, its summit reaching 25 km and the diameter at the base of the volcano amounting to 600 km. Also, fossil thermal-spring waters were probably found [12]. However, according to the cratering dating, the age of the most recent volcano calderas exceeds 100 million years [13], and a mapping thermal radiometer on Mars Observer, specially intended for searching for 'hot-spots', has not detected them [14]. Are there signs of mantle convection and volcanism?

The rarefied atmosphere of Mars does not reduce the importance of climate as a key factor determining conditions on its surface, which has largely formed the present-day relief

**O I Korablev** Space Research Institute, Russian Academy of Sciences, Moscow, Russian Federation
E-mail: korab@iki.rssi.ru

Uspekhi Fizicheskikh Nauk 183 (7) 762 – 769 (2013)
DOI: 10.3367/UFNr.0183.201307h.0762
Translated by M Sapozhnikov; edited by A M Semikhatov